Zuerst erschienen in: Applied Physics Letters 86 (2005) 072102

Magnetoresistance in $Ag_{2+\delta}Se$ with high silver excess

M. von Kreutzbruck[a)]
Institut für Angewandte Physik, Justus-Liebig-Universität Gießen, Heinrich-Buff-Ring 16, D-35392 Gießen, Germany

B. Mogwitz
Physikalisch-Chemisches Institut, Justus-Liebig-Universität Gießen, Heinrich-Buff-Ring 58, D-35392 Gießen, Germany

F. Gruhl
Institut für Angewandte Physik, Justus-Liebig-Universität Gießen, Heinrich-Buff-Ring 16, D-35392 Gießen, Germany

L. Kienle
Max-Planck-Institut für Festkörperforschung, Heisenbergstraße 1, D-70569 Stuttgart, Germany

C. Korte and J. Janek
Physikalisch-Chemisches Institut, Justus-Liebig-Universität Gießen, Heinrich-Buff-Ring 58, D-35392 Gießen, Germany

In the present study, we investigated the galvanomagnetic transport properties of polycrystalline Ag_xSe thin films with silver excess in the range from $x=1.5$ to 18. The results prove that the silver excess controls the transition from linear magnetoresistance (MR) behavior to the quadratic ordinary MR and the temperature for the metal–semiconductor transition. Analyzing the MR effect by Kohler's rule and comparing the results with the field-free resistivity we observe for $2<x<2.3$ a steep rise of the product of mean free path and electron concentration ($\lambda \cdot n^{2/3}$). We interpret this result as a consequence of the percolation of nanoscale silver networks within the semiconducting matrix, i.e., as a consequence of the two-phase character of the system.

For many years narrow gap semiconductors were of little or no concern to the field of magnetosensors. Since the appearance of an unusual linear and large magnetoresistance (MR) effect in the narrow gap (diamagnetic) silver chalcogenides $Ag_{2+\delta}Se$ and $Ag_{2+\delta}Te$ shown by Xu *et al.* in 1997[1] this has changed, and it seems possible to establish new routes for the design of magnetoresistive sensors.[2] Xu *et al.* showed that $Ag_{2+\delta}Se$ provides a linear MR effect of 370% at 4.5 K and more than 100% at room temperature ($B=5.5$ T). Manoharan *et al.*[3] found a MR effect of 250% at 4.2 K, but the linear MR field dependence was observed only for fields larger than 3 T (see also Ogorelec *et al.*[4]). Recently, Husmann *et al.*[5] successfully used $Ag_{2+\delta}Se$ as a high field sensing material as it did not show saturation up to pulsed fields of 55 T. It should be noted that qualitatively comparable results have been reported for bulk and thin film samples of $Ag_{2+\delta}Te$.[6–10] As a key to the unusual MR properties of $Ag_{2+\delta}Se$ the Hall mobility and the concentration of electronic charge carriers have been identified by several authors.[1–4,11] However, the equilibrium composition regime of homogenous α-$Ag_{2+\delta}Se$ (α denotes the orthorhombic phase stable at temperatures $T<405$ K) with its clear-cut defect chemistry is limited to $\delta_{max}(\text{hom})=8\times10^{-5}$ at room temperature and to $\delta_{max}(\text{hom})=3.3\times10^{-5}$ at 170 K (with $\delta_{max}(\text{hom})$ we denote the maximum homogeneous silver excess in the equilibrium phase).[12–16] For homogenous α-$Ag_{2+\delta}Se$ with $\delta<\delta_{max}(\text{hom})$ neither large MR effects nor linear MR behavior could be found, and the ordinary magnetoresistance effect within a two-band model is sufficient to describe the MR behavior.[17]

Only a silver metal distribution, being inhomogeneous on the nanoscale, seems to be able to explain the unusual MR behavior of silver-rich silver selenide. Macroscopic inclusions, with diameters at least on the micron scale, do not influence the MR behavior.[18] Accordingly, Abrikosov developed a theory based on the assumption of silver precipitates as small metal clusters on an atomic scale dispersed in a semiconducting matrix, to describe the linear MR phenomenon.[19] For inhomogeneous gapless semiconductors with a linear energy spectrum he predicts a linear and temperature independent MR effect which he calls quantum magnetoresistance.

In the present study, we investigated the resistivity and MR effect of polycrystalline Ag_xSe thin films in a broad range of composition for $1.5<x<18$ at room temperature and below. We prepared thin films with a thickness of 150 nm both by thermal evaporation (PVD) and by pulsed laser deposition (PLD) of stoichiometric silver selenide, which has been prepared by co-melting of the elements (99.999% purity). Films with an area of 10×10 mm^2 were deposited on fused silica substrates at a temperature of 120 °C. The thickness was determined in situ via a quartz microbalance. High-resolution scanning electron microscopy proved that samples produced by PLD showed a somewhat lower porosity and more homogeneous morphology than PVD samples. The latter consisted of grains with a size ranging between 200 and 500 nm. Energy dispersive x-ray analysis (EDX) was used for the composition analysis. The resistance and MR effect of the films was measured by a standard

a)Electronic mail: marc.v.kreutzbruck@physik.uni-giessen.de

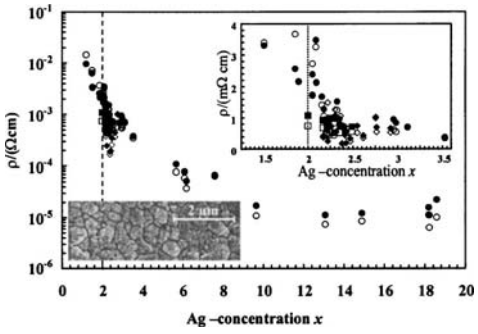

FIG. 1. Specific resistance ρ of Ag_xSe thin films as a function of the metal content x. Films made by PVD (150 nm thick): ○ (4,2 K), ● (300 K), PVD (260 nm): □ (4,2 K), ■ (300 K) and PLD (100–600 nm): ◇ (4,2 K), ◆ (300 K). Upper inset: Specific resistance ρ for silver excess up to $x=3.5$. Lower inset: REM micrograph of a PVD film surface ($x=2.22$).

four-probe method. The magnetic field was applied by a 17 T superconducting magnet system (Oxford Instruments) with temperature control ranging from 2 to 300 K (Cernox thermometer).

We plot in Fig. 1 the resistivity as a function of the metal content x for both PVD and PLD thin films (x specimens), showing a decrease in the resistivity ρ over more than three orders of magnitude from about 10 mΩ cm ($x=1.5$) down to about 10^{-2} mΩ cm ($x=18$). For metal contents only slightly higher than the stoichiometric composition at $x=2$ the graph shows a strong resistivity drop up to $x=2.3$, followed by a plateau ranging up to approximately $x=3.5$. For silver concentrations larger than $x=3.5$ again ρ decreases, converging steadily towards the resistivity limit of pure Ag (1.6 $\mu\Omega$ cm at 300 K).

To substantiate this unusual resistivity behavior we make use of the Kohler rule (KR), which states that the magnetoresistance $\Delta\rho/\rho_0$ is an universal function of the magnetic field H normalized by ρ_0 [$\Delta\rho/\rho_0=f(H/\rho_0)$]. The KR is well obeyed for most metals and half metals in broad temperature ranges, and deviations from KR indicate the presence of additional electron scattering mechanisms with a modified relaxation time τ along the orbit path on the Fermi surface. As an example we illustrate in Fig. 2 the Kohler plot for a sample with $x=2.30$. For fields beyond 3 T the MR is scaled by H. The data for temperatures ranging between 50 and 150 K have approximately the same slope which implies that KR holds. For higher temperatures large deviations from KR occur. For silver concentrations slightly higher then the stoichiometric concentration ($x<2.5$) we found a linear MR for

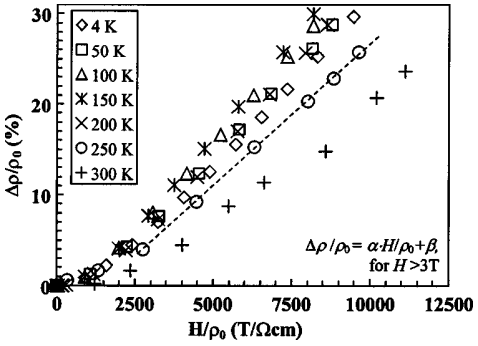

FIG. 2. Kohler plot: MR effect as a function of H/ρ_0 for a Ag_xSe sample with $x=2.30$ and magnetic fields up to 12 T.

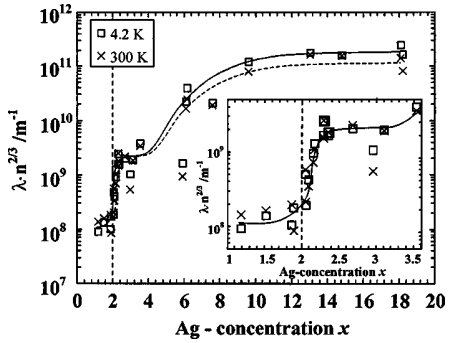

FIG. 3. Product of mean free path λ and charge carrier concentration with exponent 2/3 as a function of the metal content x. Inset: $\lambda\cdot n^{2/3}$ for silver excess up to $x=3.5$.

fields larger than 2 T, whereas for $x<2$ or $x>2.5$ the linear MR was observed for fields ranging from 4 to 10 T. The linear MR behavior of Ag_xSe allows for a linear approach $\Delta\rho/\rho_0=\alpha\cdot H/\rho_0+\beta$ at higher fields. For free electrons the quantity H/ρ_0 can be expressed as a function of the electronic mean free path λ and the radius of the cyclotron orbit r_c with $H/\rho_0=(\lambda/r_c)\cdot n\cdot e$, where n denotes the number of electrons per unit volume. Using the expression for the electron orbit radius $r_c=\hbar(3\pi^2\cdot n)^{1/3}/(e\cdot H)$, one obtains a linear relation between $\lambda\cdot n^{2/3}$ and the measurable zero field conductivity σ_0, i.e., $\lambda\cdot n^{2/3}=\hbar(3\pi^2\cdot n)^{1/3}\cdot\sigma_0/e^2$. Our linear approximation for the MR effect is then also transformed into a linear relation with $\lambda\cdot n^{2/3}$:

$$\frac{\left(\frac{\Delta\rho}{\rho_0}-\beta\right)}{\alpha\cdot H}\cdot\frac{\hbar\cdot(3\pi^2)^{1/3}}{e^2}=\lambda\cdot n^{2/3}.$$

We thus expect an inverse behavior with respect to Fig. 1. By determining the slope α, β, and $\Delta\rho/\rho_0$ at $H=12$ T for each PVD sample we can plot $\lambda\cdot n^{2/3}$ as a function of the metal content x. Figure 3 shows that $\lambda\cdot n^{2/3}$ exhibits (both at 4.2 and 300 K) a distinct steep rise in the regime ranging from $x=2$ and $x=2.3$. Corresponding to Fig. 1 we find for $x>2.3$ a plateau for metal contents of approximately up to $x=3.5$ which then gradually inclines for higher Ag concentration towards to the limit for silver of 8.6×10^{11} m^{-1} [$\lambda=57$ nm and $n=5.85\times10^{28}$ m^{-3} (at 300 K)].

We interpret our results as a clear indication of the occurrence of a twofold percolation phenomenon. The concentration of silver clusters or nanoscale inclusions increases along with the increase in metal content after leaving the composition regime of the homogeneous silver selenide α phase. Experimental evidence for the existence of nano scale silver "inhomogeneities" is given by Ohachi, reporting silver atom trapping at non-equilibrium defects such as dislocations and grain boundaries.[20,21] One can expect these clusters or inclusions to be located primarily along grain boundaries and dislocations. Nanoscale silver clusters are interconnected if the volume fraction of silver with respect to the effective grain boundary and dislocation volume is higher than about 30% (percolation threshold at $\delta\approx0.05$). This boosts the amount of current paths on certain surfaces of grains and dislocations. For higher silver excess ($\delta\approx0.25$) the effective volume of the grain boundaries and dislocations is completely filled with Ag, corresponding to the saturation and beginning of the plateau in Figs. 1 and 3. Any further in-

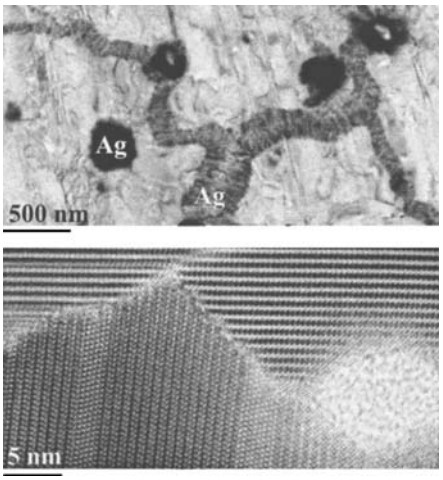

FIG. 4. Top: Coexistence of silver nanoparticles and silver lamellas (silver paths) for $(Cu,Ag)_2Se$. Bottom: HRTEM micrograph of lamellas and grains of Ag_2Se.

crease of the silver excess will cause metal clusters to grow inside the grain as well. But these clusters are still nonchained and thus have—contrary to the silver paths along the grain surfaces—a negligible effect on the sample's conductivity. That changes when the three-dimensional-percolation threshold is exceeded by an approximately 30% volume fraction of silver hosted in the semiconducting matrix. This silver amount corresponds to $\delta \approx 1.3$ which concurs with the point we observe in Fig. 3 at $x=3.3$, at which the conductivity again starts to rise. For silver concentrations higher than the percolation threshold ($\delta > 1.3$) the precipitated Ag clusters begin to form a three-dimensional network in the whole bulk and the total resistance converges to the resistance of metallic silver.

High-resolution transmission electron microscopy (HRTEM)[22] and selected area electron diffraction were performed to investigate the complex real structure of additionally prepared 30-nm-thick PLD–Ag_xSe films. The morphology of the films is characterized by thin lamellas of the low temperature polymorphs of Ag_2Se[23] and show polysynthetic twinning with rectangular orientations of the twinned domains. Additionally, an incongruent intergrowth of randomly orientated grains of the low temperature phases occur with significant misfit of the structures at the grain boundaries, see Fig. 4 bottom. Nanoscale silver precipitates in the form of nanoparticles (average size $\sim$100 nm) were detected on the surface of the Ag_2Se films by EDX mapping. Besides nanoparticles, silver lamellas being consistent with our model of silver paths had been observed in the case of Ag_2Se films that contain copper impurities. As depicted in Fig. 4 top, the orientation of the silver lamellas and the $(Cu,Ag)_2Se$ matrix is random, as the silver aggregates between randomly orientated grains of $(Cu,Ag)_2Se$. A detailed study of the microstructure by electron microscopy is in progress.

Our model of a nanoscale percolation network relates directly to recent theoretical work by Parish and Littlewood who attempt to explain the linear MR effect in the silver chalcogenides by a simulation of a random network of microscopic (four-terminal) resistors.[24,25] For such a heterogeneous conductivity distributions they obtain a linear positive and nonsaturating MR effect which, however, still appears at much higher critical fields than the linear MR effect in $Ag_{2+\delta}Se$.

[1] R. Xu, A. Husmann, T. F. Rosenbaum, M.-L. Saboungi, J. E. Enderby, and P. B. Littlewood, Nature (London) **390**, 57 (1997).
[2] S. A. Solin, Tineke Thio, D. R. Hines, and J. J. Heremans, Science **289**, 1530 (2000).
[3] S. S. Manoharan, S. J. Prasanna, D. Elefant Kiwitz, and C. M. Schneider, Phys. Rev. B **63**, 212405 (2001).
[4] Z. Ogorelec, A. Hamzic, and M. Baletic, Europhys. Lett. **46**, 56 (1999).
[5] A. Husmann, J. B. Betts, G. S. Boebinger, A. Migliori, T. F. Rosenbaum, and M. L. Saboungi, Nature (London) **417**, 421 (2002).
[6] I. S. Chuprakov and K. H. Dahmen, Appl. Phys. Lett. **72**, 2165 (1998).
[7] B. Q. Liang, X. Chen, Y. J. Wang, and Y. J. Tang, Phys. Status Solidi B **215**, 1145 (1999).
[8] B. Q. Liang, X. Chen, Y. J. Wang, and Y. J. Tang, Phys. Rev. B **61**, 3239 (2000).
[9] H. S. Schnyders, M.-L. Saboungi, and T. F. Rosenbaum, Appl. Phys. Lett. **76**, 1710 (2000).
[10] M. Lee, T. F. Rosenbaum, M. L. Saboungi, and H. S. Schnyders, Phys. Rev. Lett. **88**, 066602 (2002).
[11] G. Beck and J. Janek, Physica B **308–310**, 1086 (2001).
[12] U. von Oehsen and H. Schmalzried, Ber. Bunsenges. Phys. Chem. **85**, 7 (1981).
[13] G. Beck and J. Janek, Solid State Ionics (in press).
[14] C. Korte and J. Janek Z. Phys. Chem. **206**, 129 (1998).
[15] G. Beck and J. Janek (unpublished).
[16] H. Wysk and H. Schmalzried, Solid State Ionics **96**, 41 (1997).
[17] *Binary Phase Diagrams*, 2nd ed., edited by T. B. Massalski (ASM International, 1990).
[18] G. Beck, Dr. rer. nat. thesis, Justus-Liebig-Universität Giessen , Giessen 2002 (available online: http://geb.uni-giessen.de/geb/volltexte/2003/1002/).
[19] A. A. Abrikosov, Phys. Rev. B **58**, 2788 (1998).
[20] Y. Kumashiro, T. Ohachi, and T. Taniguchi, Solid State Ionics **86–88**, 761 (1996).
[21] T. Ohachi, M. Hiramoto, Y. Yoshihara, and I. Taniguchi, Solid State Ionics **51**, 191 (1992).
[22] Philips CM 30, 300 kV, LaB_6 cathode.
[23] J. R. Günter and P. Keusch, Ultramicroscopy **49**, 293 (1993).
[24] M. M. Parish and P. B. Littlewood, Nature (London) **426**, 162 (2003).
[25] T. F. Rosenbaum, Nature (London) **426**, 135 (2003).